# The Effects of Rotation on the Nonlinear Reflection of Internal Waves from a Slope

S. A. THORPE

*School of Ocean and Earth Science, Southampton Oceanography Centre, Southampton, United Kingdom*

(Manuscript received 7 December 1998, in final form 27 August 1999)

ABSTRACT

The effect of rotation on the nonlinear reflection of internal waves from a sloping boundary is examined. The waves propagate at an angle $\beta$ to the horizontal in an ocean of locally uniform buoyancy frequency $N$, and the boundary slopes at angle $\alpha$ to the horizontal. The following modifications are found when rotation is taken into account: 1) The modulus of the Lagrangian alongslope drift caused by the waves may be increased by an order of magnitude, and the level above the boundary at which the greatest drift is generated is no longer at $z = 0$, but depends on $f/N$ where $f$ is the Coriolis frequency, and the direction of the drift close to the boundary may be reversed. 2) Eulerian upslope currents associated with reflection are increased by a factor $O(2)$. Particularly large currents are found to be generated for incident waves travelling almost directly downslope and when $\beta > \alpha$. 3) The mean density and the vertical displacement of isopycnals caused by the waves are increased, possibly by factors $O(2)$. 4) The generation of density fronts near the boundary is only slightly affected, except possibly when the incident wave direction $\beta$ is close to values at which the second-order wave components are near critical when $f/N = 0$. Here rotation reduces the tendency for fronts to form.

## 1. Introduction

Present interest in the interaction of internal waves and topography stems from observations of enhanced mixing near topography and speculation that processes involving internal waves may be its cause (Polzin et al. 1997; Eriksen 1998, Toole et al. 1997). The work reported here derives from a conjecture that rotation may be of importance, particularly that near-inertial internal gravity waves reflecting from sloping boundaries may result in nonlinear effects that have different consequences and perhaps are of greater magnitude than for relatively short period waves in which the effects of rotation are negligible.

There are several processes that are known to result from the nonlinear interaction between internal waves incident on a sloping boundary and their reflected components. In the case considered here the waves propagate toward the sloping boundary through a fluid with constant buoyancy frequency $N$, and the boundary is plane. This simplistic representation includes much of the essential physics and is sufficient for a quantified study of wave effects, including (i) a local increase or decrease in the mean density field at points fixed in space, or equivalently a setup or setdown, respectively, of isopycnal surfaces (Wunsch 1971; Thorpe 1987); (ii) the generation of upslope Eulerian currents that, although they contribute to the currents which might be measured by a moored current meter, are balanced by an equal and opposite Stokes drift so that the resulting Lagrangian flow is zero (Thorpe 1987); (iii) the generation of alongslope Lagrangian flows when the incident waves approach the slope obliquely but do not loose energy (Thorpe 1997), or Eulerian flows when the waves break or loose energy (Hogg 1971; Thorpe 1998a; Dunkerton et al. 1998); (iv) the generation of density fronts that travel up the slope with the speed of wave phase advance (Thorpe 1992, 1999; Dunkerton et al. 1998); and (v) resonant interaction, which in some circumstances may lead to breaking (Thorpe 1987). Resonant interaction at second and higher orders occurs when particular relations are satisfied between the angle of the sloping boundary to the horizontal, $\alpha$, and the angle which the group velocity vector makes with the horizontal, $\beta$ (Thorpe 1997, 1998b).

In cases (i)–(iv) nonlinear, as well as linear, effects are found to increase when the internal waves are close to ''critical'' (Phillips 1966; Eriksen 1982, 1985), that is, when $\alpha$ is close to $\beta$. The upslope Eulerian current (ii), and Lagrangian flow (iii), are however generally small, order 1 cm $s^{-1}$ or less, in the absence of rotation.

In the case (iv) of density front formation, it has recently been noticed that, in the absence of rotation, nonlinear effects are also large when *harmonics* of the incident wave frequency, generated by the interaction of the incident and reflected wave, are themselves critical (Thorpe 1999). Neglecting rotation, the wave frequency

*Corresponding author address:* Dr. Steve A. Thorpe, Bodfryn, Glanrafon, Llangoed, Anglesey LL58 8PH, United Kingdom.
E-mail: oss413@sos.bangor.ac.uk

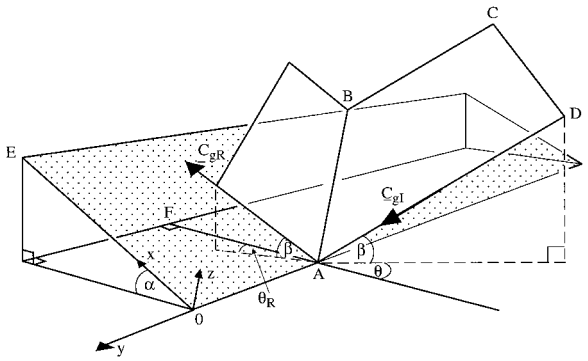


FIG. 1. The reflection of an incident internal wave with constant phase surface ABCD inclined at angle $\beta$ to the horizontal, from a sloping plane boundary AOEB (stippled), inclined at angle $\alpha$. The group velocity of the internal wave, $C_{gI}$ lies in the constant phase plane directed down its line of steepest descent, and is therefore also inclined at angle $\beta$ to the horizontal. Its projection onto the horizontal makes an angle $\theta$ to the horizontal line in a plane normal to isobaths AO; $\theta$ defines the azimuthal angle of incidence of the wave to the slope. A constant phase surface of the reflected wave with group velocity $C_{gR}$ is shown, also inclined at angle $\beta$ to the horizontal and intersecting the plane boundary at AB, but with a reflected angle $\theta_R$. In the case shown, with $\theta < \pi/2$, the angle of the reflected wave $\theta_R$ is $< \theta$ (see Eriksen 1985) and, on reflection, the wave direction turns toward the line of greatest slope up the plane boundary. The incident phase plane advances upward so that its intersection AB with the plane moves up and along the slope toward E and, correspondingly, the constant phase plane of the reflected wave moves downward. The axes have origin O on the plane boundary, and are x up a line of greatest slope, y horizontal along a constant depth contour on the boundary, and z upward and normal to the sloping boundary.

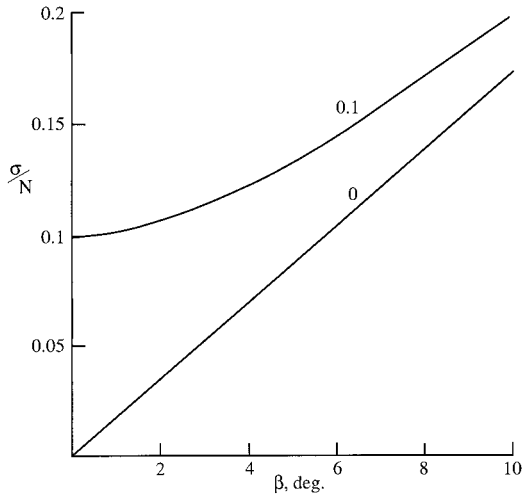


FIG. 2. The variation of $\sigma/N$ with propagation angle, $\beta$, for $f/N = 0$ and 0.1.

$\sigma$ is related to the wave group propagation direction $\beta$ by the relation $\sigma = Ns_\beta$; that is, the direction is $\beta = \sin^{-1}(\sigma/N)$. (Here and later $s_\beta$, $c_\alpha$, etc., stand for $\sin\beta$, $\cos\alpha$, etc., respectively.) The first harmonic, frequency $2\sigma$, therefore travels in direction $\sin^{-1}(2\sigma/N)$, or $\sin^{-1}(2s_\beta)$, which is the same as that of the slope if $2s_\beta = s_\alpha$, or when $\beta = \sin^{-1}[(s_\alpha)/2]$. Higher harmonics will be critical if $\beta = \sin^{-1}[(s_\alpha)/n]$, $n = 3, 4, \cdots$.

Such angles of wave propagation, $\beta$, and therefore incident waves, are possible whatever the slope angle $\alpha$. This is not true in a rotating system. Then

$$\sigma^2 = N^2 s_\beta^2 + f^2 c_\beta^2, \tag{1}$$

(Gill 1982), where $f$ is the Coriolis frequency, which, for sake of argument and because it is generally so in the ocean, is taken to be less than $N$. The first harmonics travel in a direction equal to $\alpha$ if $(2\sigma)^2 = N^2 s_\alpha^2 + f^2 c_\alpha^2$ or, from (1), when $\beta = \sin^{-1}\{[s_\alpha^2 - 3f^2/(N^2 - f^2)]^{1/2}/2\}$. Solutions are only possible when

$$\alpha > \sin^{-1}\{[3f^2/(N^2 - f^2)]^{1/2}\}. \tag{2}$$

There is therefore a minimum slope at which such harmonic, nonlinear, critical slope effects may be expected. For example, if $f/N = 0.1$, the minimum slope of the boundary is 10.02°; rotation may have significant physical consequences, even if $f/N \ll 1$.

The effects of rotation have already been considered and quantified in case (v) (Thorpe 1997). Previous results for cases (i) to (iv) are extended here to quantify the effects of rotation in the simplest case in which the waves do not break and lose momentum at the boundary but reflect perfectly, retaining their frequency but changing their wavenumber and amplitude to produce the effects described below.

## 2. Analysis

The ocean is characterized here by $N$, $f$, and its boundary slope $\alpha$. The incident waves have downward propagation direction $\beta$, amplitude $A$ (the amplitude of isopycnal disturbances), horizontal and vertical wavenumbers $K$ and $M$ (with $\tan\beta = K/M$), steepness $s = AM$, and azimuthal direction relative to the slope, $\theta$ (i.e., the angle between the projection of the group velocity vector onto the horizontal and a horizontal line normal to isobaths on the slope; Fig. 1). The angle $\theta$ is zero when the incident waves propagate in a plane normal to the slope, and 90° when the waves travel in a vertical plane parallel to contour lines on the slope. Equation (1) shows that $\sigma/N$ varies with $\beta$ when $f/N$ is held constant. Figure 2 shows this variation for $f/N = 0$ and 0.1. The frequency $\sigma$ tends to $f$ as $\beta$ tends to zero. The angle $\beta$, rather than the wave frequency $\sigma$, is used to characterize the waves since it is the angle ratio $(\alpha - \beta)/\beta$, which provides a measure of how close the waves are to being critical and which is crucial in determining the magnitude of many nonlinear effects. If $\sigma$ is held constant, then $\beta$ will vary with $f/N$ and so too will $(\alpha - \beta)$.

### a. First-order solution

The $(x, y, z)$ axes are chosen with $z = 0$ on the sloping boundary, $x$ up the line of greatest slope, and $y$ hori-

zontally along the slope (Fig. 1). The analysis follows that described by Thorpe (1997). The governing equations are given in appendix A and a pair of *exact* solutions of the equations of motion and continuity are presented in appendix B. Together these satisfy the boundary condition $w = 0$ at $z = 0$, and individually they represent the incident and reflected waves. The solutions are for the $(x, y, z)$ velocity components, $(u, v, w)$, and for density $\rho$, with subscripts $I$ and $R$ to indicate the incident and reflected waves, respectively. The density and velocity components are composed of $\sin(kx + ly + m_i z - \sigma t)$ and $\cos(kx + ly + m_i z - \sigma t)$ terms, with $m_i = m_I$ or $m_R$, the coefficients of which are written as $\rho_{cI}$, $\rho_{sI}$, etc., where $s$ and $c$ stand for sin and cos, respectively. All are linearly proportional to the incident wave amplitude $A$.

The sum of this pair of solutions gives the first-order motion and density fields. At $z = 0$, the density is $\rho_0(1 - N^2 x s_\alpha/g) + q_1 \sin(kx + ly - \sigma t + \phi_{\rho 1})$, where $q_1 = [(\rho_{cI} + \rho_{cR})^2 + (\rho_{sI} + \rho_{sR})^2]$ and $\tan\phi_{\rho 1} = (\rho_{cI} + \rho_{cR})/(\rho_{sI} + \rho_{sR})$; $\phi_{\rho 1} = 0$ if $f/N = 0$ (appendix B). It is readily shown that there are no mean drifts associated with the exact solutions separately; only when the incident and reflected waves coexist, as they must near the boundary, are Lagrangian drifts generated through their interaction.

### b. Second-order solution

The first-order velocity components can be used to obtain the alongslope Lagrangian drift $V_L$, for which an expression is given in Thorpe (1997; appendix C). This is described in section 3a. The second-order components of velocity $(u_2, v_2, w_2)$ and density $\rho_2$ are found in the conventional way by solving the vorticity and continuity equations with the first order solutions substituted into the nonlinear terms, as outlined in appendix C. The *II* and *RR* product terms vanish exactly leaving terms sinusoidal in $\chi_+ = [2(kx + ly - \sigma t) + (m_I + m_R)z]$ or in $\chi_- = (m_R - m_I)z$. The $\chi$ components are steady Eulerian current components or density perturbations, which vary sinusoidally with distance $z$ from the slope with scale $2\pi/(m_I - m_R)$. Three second-order terms are found and discussed in section 3b–d. These are, respectively, the steady Eulerian upslope component of current $U$, the mean density perturbation $II$ (proportional to the setup of isopycnals), and the periodic density fluctuation $\rho_2$.

## 3. Results

The results described below have been computed numerically from the second-order solutions and are shown graphically for the bottom slope angle, $\alpha = 5°$, a value typical of oceanic slopes, and at $f/N = 0$ and 0.1 so that the effects of including rotation may be assessed.

### a. Lagrangian alongslope drift, $V_L$

The alongslope Lagrangian drift is nondimensionalized with $N/K$ and scaled with $s^2$ so that $V_L/[s^2(N/K)] = \langle V_L\rangle \sin[(m_R - m_I)z + \phi_L]$. The variation of $\langle V_L\rangle$ with $\theta$ at various $\beta$ and $f/N = 0$ is shown in Fig. 3a. Here $\langle V_L\rangle$ is zero at $\theta = 0$ and $\pi$ and has a maximum (when $\alpha < \beta$) or minimum (when $\alpha > \beta$) at $z = 0$; $\langle V_L\rangle$ tends to 0 as $\theta$ tends to $-\cos^{-1}(s_\beta c_\alpha/s_\alpha c_\beta)$, possible only when $\beta < \alpha$. In this $\theta$ limit the internal wave group velocity vector becomes parallel and tangential to the sloping boundary (Thorpe 1999). For comparison, Fig. 3b shows $\langle V_L\rangle$ at $f/N = 0.1$. Here $\langle V_L\rangle$ has a maximum at $\theta = 0$ and values that are an order of magnitude greater than those found when $f/N = 0$ (Fig. 3a). When $f/N = 0$, the phase angles, $\phi_L$, equal $\pi/2$ if $\beta > \alpha$ or $\pi/2$ if $\beta < \alpha$ (Thorpe 1997). For comparison, Fig. 3c shows the phase angles $\phi_L$ when $f/N = 0.1$. The vertical arrows mark the values of $\theta$ at which, for the specified $\beta$, the group velocity vector is parallel to the slope (where $\langle V_L\rangle = 0$ when $\alpha > \beta$, see above) or, when $\alpha < \beta$, where the lines of constant wave phase on the slope are parallel to a line of greatest slope. Here $\theta = -\cos^{-1}(s_\alpha c_\beta/c_\alpha s_\beta)$, the alongslope wavelength tends to zero, and $k/l$ tends to infinity; the limit is one in which $\langle V_L\rangle$ tends to a finite, nonzero, limit. When $f/N \neq 0$, the phase $\phi_L$ is generally such that the position of the maximum drift is no longer at $z = 0$ but above the boundary at height $z_{\max} = (\pi/2 - \phi_L)/(m_R - m_I)$. Figures 3a,b show that, as $\theta$ tends to zero, the behavior of $\langle V_L\rangle$ depends on $f/N$. At $\beta = 6°$, $\langle V_L\rangle$ has a minimum value at $\theta = 0$ when $f/N$ is less than about 0.015. There is however a maximum at $\theta = 0$ for values of $f/N > 0.02$ (at least up to $f/N = 0.1$).

Figure 4 shows how $\langle V_L\rangle$ and $\phi_L$ vary with $f/N$ when $\theta = 40°$. The phase changes rapidly as $f/N$ increases from 0 and $\langle V_L\rangle$ increases monotonically with $f/N$. The Lagrangian drift at $z = 0$, $\langle V_L\rangle \sin\phi_L$, changes sign at about $f/N = 0.05$ for $\beta = 4°$ (Fig. 4a). Figure 5 shows the maximum drift at $z = 0$, $\max\langle V_L\rangle$, as a function of $\beta$. When $f/N = 0$, the largest drifts at $z = 0$ occur at increasing values of $\theta$ as $\beta$ increases; $\max\langle V_L\rangle$ is at $\theta = 41°$ when $\beta = 2°$ and $\theta = 54°$ when $\beta = 8°$. When $f/N = 0.1$, however, the largest values are at slowly decreasing $\theta$ when $\beta$ increases and is less than $\alpha$ (the $\max\langle V_L\rangle$ is at $\theta = 56°$ when $\beta = 2°$ and at $\theta = 54°$ when $\beta = 4°$), but at slowly increasing $\theta$ when $\beta$ increases and is greater than $\alpha$ ($\max\langle V_L\rangle$ is at $\theta = 52°$ when $\beta = 6°$ and at $\theta = 54°$ when $\beta = 8°$.) Figure 5 shows that larger values of $\max\langle V_L\rangle$ are found for $f/N = 0.1$ than at $f/N = 0$; the angular range in $\beta$ of the region of large drift near the critical slope, $\beta = \alpha$, is expanded. Comparison with Fig. 2 shows that the range of frequencies, $\sigma/N$, in which a particular value of $\max\langle V_L\rangle$ may be found, also increases as $f/N$ increases from 0 to 0.1.

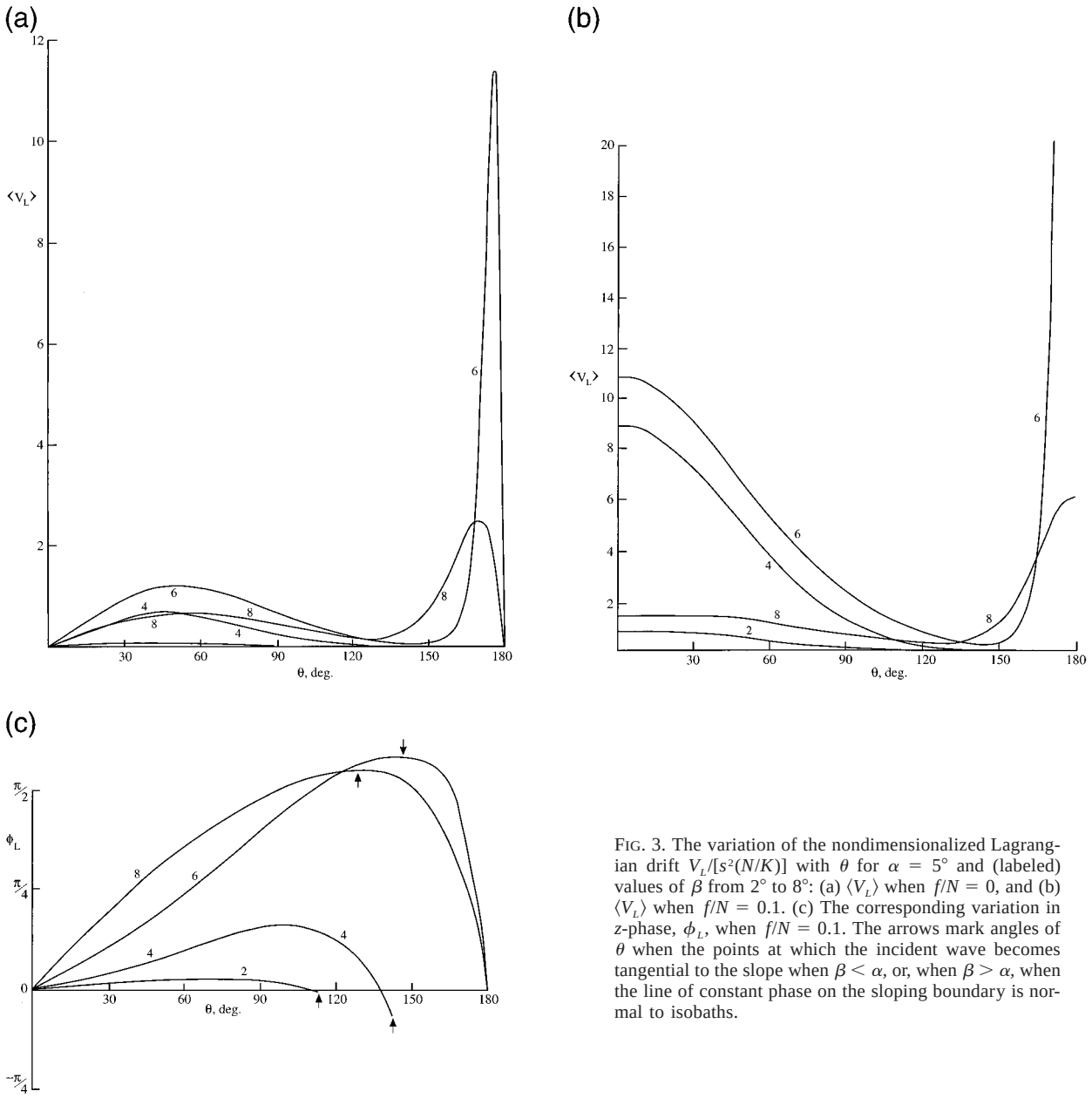


FIG. 3. The variation of the nondimensionalized Lagrangian drift $V_L/[s^2(N/K)]$ with $\theta$ for $\alpha = 5°$ and (labeled) values of $\beta$ from 2° to 8°: (a) $\langle V_L \rangle$ when $f/N = 0$, and (b) $\langle V_L \rangle$ when $f/N = 0.1$. (c) The corresponding variation in $z$-phase, $\phi_L$, when $f/N = 0.1$. The arrows mark angles of $\theta$ when the points at which the incident wave becomes tangential to the slope when $\beta < \alpha$, or, when $\beta > \alpha$, when the line of constant phase on the sloping boundary is normal to isobaths.

*b. Upslope Eulerian current, U*

The mean Eulerian upslope current component is scaled and nondimensionalized in the same way as $V_L$ so that $U/(s^2N/K) = \langle U \rangle \sin[(m_R - m_I)z + \phi_U]$. At $f/N = 0$, $\langle U \rangle = -2r\gamma s_\beta^2/(rs_\beta c_\alpha - s_\alpha c_\beta)^3$ and $\phi_U = -\pi/2$, where $r = (c_\alpha s_\beta + c_\theta c_\beta s_\alpha)/(c_\theta s_\beta c_\alpha + s_\alpha c_\beta)$ (Thorpe 1997). Figure 6a shows $\langle U \rangle$ plotted as a function of $\theta$ for various $\beta$ at $f/N = 0.1$ (full lines) and $f/N = 0$ (dashed), and Fig. 6b shows the corresponding $z$ phase. The effect of rotation is to produce only modest increases in the current magnitude and in the height of the maximum current above the boundary (i.e., $\phi_U$ is close to the nonrotating value, $-\pi/2$) except where the current is very small. Large currents are generated when the internal waves are propagating down the slope, near $\theta = \pi$. Then $\langle U \rangle$ tends to zero at the values of $\theta$ equal to the values $-\cos^{-1}(s_\beta c_\alpha/s_\alpha c_\beta)$ when $\beta < \alpha$, or $-\cos^{-1}(s_\alpha c_\beta/c_\alpha s_\beta)$ when $\alpha < \beta$, discussed in section 3a and indicated by arrows in Fig. 3c. (These values are when $r$ is 0 or tends to infinity, respectively.)

*c. Mean density, Π*

The time-averaged second-order density term is made nondimensional using the amplitude of the density var-

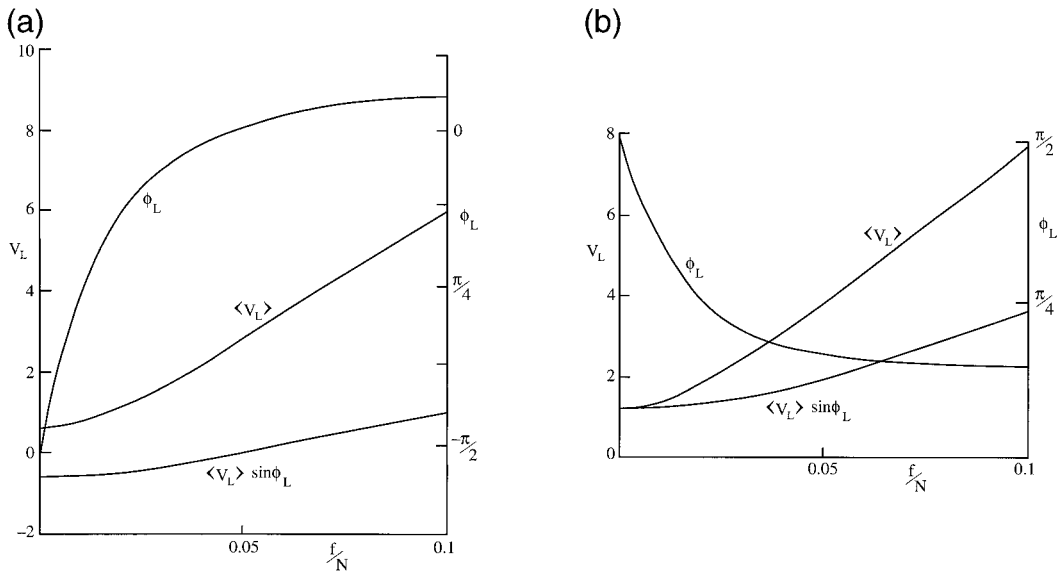


FIG. 4. The variation of the nondimensional magnitude of the alongslope Lagrangian drift $\langle V_L \rangle$ and the corresponding $z$-phase, $\phi_L$, and drift speed at $z = 0$, $\langle V_L \rangle \sin\phi_L$, with $f/N$ at $\alpha = 5°$ and $\theta = 40°$, and (a) $\beta = 4°$ and (b) $\beta = 6°$.

iations induced by the incident wave, $AN^2/g$, and scaled with $s$ so that $\Pi/(sAN^2/g) = \langle \Pi \rangle \sin[(m_R - m_I)z + \phi_\Pi]$. If $f/N = 0$, $\langle \Pi \rangle = 2c_\alpha s_\beta r^3(s_\beta c_\alpha c_\theta + s_\alpha c_\beta)/s_\beta c_\alpha r - s_\alpha c_\beta)^2$ and $\phi_\Pi = 0$ (Thorpe 1997). Figures 7a,b show the variations of the magnitude and phase of $\langle \Pi \rangle$ with $\theta$ and $\beta$. The effect of rotation is to increase the magnitude of $\Pi$ and to change the $z$ location, $z_{max}$, at which the maximum density changes occur. Here $\langle \Pi \rangle$ tends to zero at the values of $\theta$ for which the incident wave becomes tangential to the slope and has a minimum where the lines of constant phase on the slope are parallel to the lines of greatest slope.

### *d. Periodic density variations, $\rho_2$: Fronts*

The sum of the first and second order periodic terms that arise in the density at $z = 0$ can be written as $q_1 \sin(kx + ly - \sigma t + \phi_{\rho 1}) + q_2 \sin[2(kx + ly - \sigma t) + \phi_{\rho 2}]$, where the first-order term, $q_1$, is proportional to $s$, and $q_2$ is proportional to $s^2$. The ratio, $R = q_2/sq_1$, is a measure of the relative size of the second and first order terms. Their relative phase determines how they combine to contribute to distort the wave form from sinusoidal, perhaps with the formation of large density gradients or fronts. The density gradient parallel to the slope is found by taking spatial derivatives of density, while the temporal gradients are found by time derivatives. Derivatives of second-order terms introduce a multiplicative factor 2 to the ratio of relative importance, $R$. When the phase of the first-order term, $(kx + ly - \sigma t + \phi_{\rho 1})$, is zero, the phase of the second-order term is $\phi_\rho = \phi_{\rho 2} - 2\phi_{\rho 1}$. This is an indicator of the relative contribution of the second and first order density gradients. When $f/N = 0$, $\phi_\rho = \pi$ (Thorpe 1999) so that the first and second order terms are 180° out of phase. The second-order terms then produce an asymmetry in which, during a wave cycle, the density increases more rapidly than it falls, with the formation of fronts during the upslope phase of motion. These are observed in the ocean and in laboratory experiments (Thorpe 1992; Dunkerton et al. 1998). They are most intense when the relative contribution of the second-order terms is large, that is, when $R$ is large.

Figures 8a,b show the variation of $R$ with $\theta$ at $f/N = 0$ and 0.1, respectively, and Fig. 8c shows $\phi_\rho$ when $f/N = 0.1$. When $\beta < \alpha$, $R$ decreases to zero as $\theta$ increases to about $\theta = 150°$. If $\beta > \alpha$, $R$ has a minimum near $\theta = 150°$, increasing rapidly with $\theta$ for larger $\theta$. Comparison of Figs. 8a and 8b shows that generally increasing $f/N$ from zero has only a minor effect. At

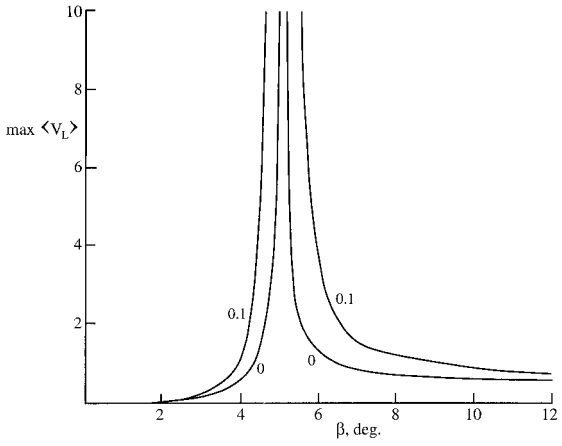


FIG. 5. The variation of the maximum nondimensional alongslope Lagrangian drift, max$\langle V_L \rangle$, at $z = 0$ when $\alpha = 5°$ and when $f/N = 0$ or 0.1, as indicated by labels.

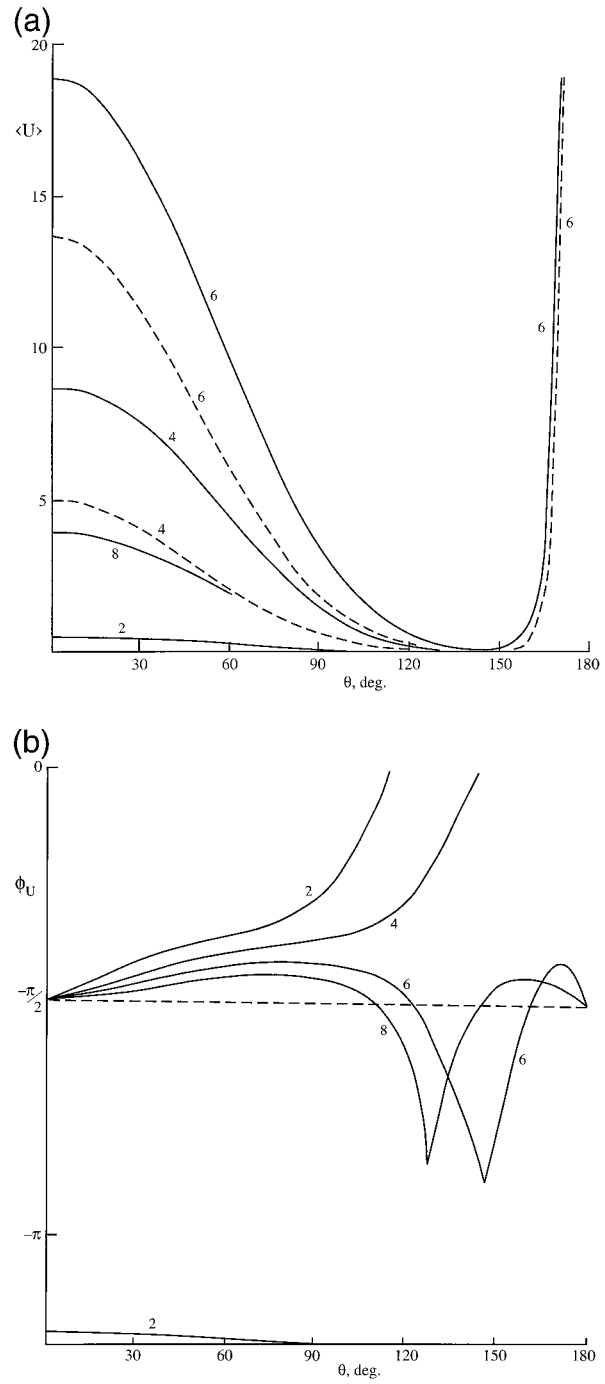


FIG. 6. The variation of the nondimensionalized upslope component of the Eulerian velocity, $U/[s^2(N/K)]$, with $\theta$ at $\alpha = 5°$ and for various values of $\beta$ (labeled): (a) the modulus of the component $\langle U \rangle$. The full curves are for $f/N = 0.1$ and the dashed curves are for $f/N = 0$. (b) The corresponding $z$-phases, $\phi_U$, when $f/N = 0.1$. The phase is $-\pi/2$ when $f/N = 0$ (dashed).

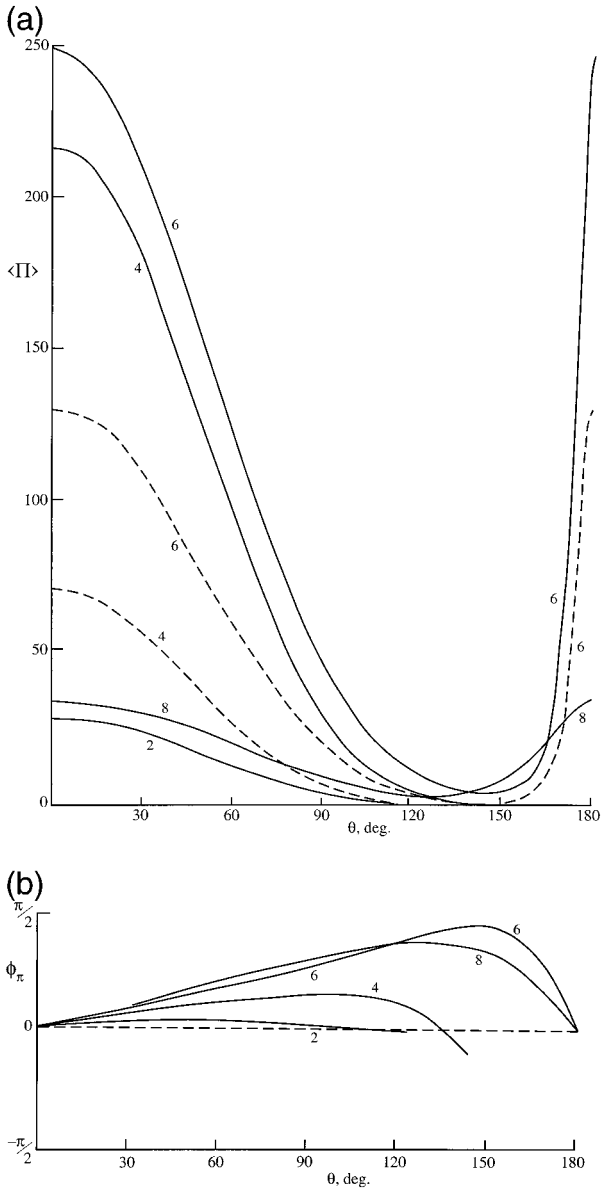


FIG. 7. The variation of the nondimensionalized mean density changes, $\Pi/(AN^2/g)$, with $\theta$ at $\alpha = 5°$ and at various $\beta$ (labeled): (a) $\langle \Pi \rangle$, the modulus of the density variation. The full curves are for $f/N = 0.1$ and the dashed curves are for $f/N = 0$. (b) The corresponding $z$-phases, $\phi_\Pi$, when $f/N = 0.1$. The phase is $\pi$ when $f/N = 0$.

$\beta = 4°$, however, the values of $R$ when $f/N = 0$ exceed those when $f/N = 0.1$. The reason for this is apparent in Fig. 9, which shows the variation of $R$ with $\beta$ at $f/N = 0$ and 0.1, and at the fixed angle of incidence, $\theta = 20°$. When $f/N = 0$, $R$ tends to infinity for values of $\beta$ near 2.5°, but there is no corresponding singularity in $R$ when $f/N = 0.1$. This is in accord with the conclusion in section 1 that, in the absence of rotation, nonlinear effects are large near $\beta = \sin^{-1}(s_\alpha/2)$ (or, if $\alpha$ is small, when $\beta$ is approximately equal to $\alpha/2$), whereas no corresponding singularity is possible when $f/N = 0.1$ unless $\alpha > 10.02°$. Large values of $R$ are found for values of $\beta \approx \alpha$ when $\theta$ is near 0° and, when $\beta > \alpha$, for $\theta$ near 180°. In the range of $\theta$ for which $R$ attains these large values and when $f/N = 0.1$, Fig. 8c shows that

$\phi_\rho$ is near $\pi$, the same value of $\phi_\rho$ as when $f/N = 0$. In general, therefore, the effect of rotation does not significantly effect either the enhancement of the negative density gradients by the second-order terms or the consequent formation of fronts. The exception is when harmonics are near their critical slopes.

## 4. Discussion

The main conclusions of this study of the effects of rotation on processes associated with internal wave reflection from a uniform sloping boundary are that, as a consequence of rotation,

1) the modulus of the Lagrangian alongslope drift, $V_L$, may be increased by an order of magnitude, the level above the boundary at which the maxima in the drift are found is no longer at $z = 0$, but depends on $f/N$, and the direction of the drift close to the boundary may be reversed (section 3a);
2) the Eulerian upslope currents, $U$, may be increased by a factor $O(2)$. Large currents are generated for incident waves in direction $\theta$ near 180° when $\beta > \alpha$ (section 3b);
3) the mean density and the setup of isopycnals are increased, possibly by factors $O(2)$ (section 3c); but
4) the generation of density fronts near the boundary is little affected, except near the incident wave directions, $\beta$, where, if $f/N = 0$, the second-order terms are near-critical (section 3d).

Of these, the most significant consequence of rotation is the enhancement of the Lagrangian alongslope drift resulting from wave reflection. A drift is generated even when the angle of incidence $\theta$ is zero, that is, when the waves approach the slope normally. Values of the nondimensional drift, $\langle V_L \rangle = |V_L|/[s^2(N/K)]$ of order 10 are found when $\theta$ is less than 30° and $\beta$ within one degree of the slope inclination, $\alpha$ (Fig. 3b). When $\alpha = 5°$ and $f/N = 0.1$ (as in Fig. 3b), $\sigma/N$ is about 0.13 (Fig. 2), so $|V_L|$ is about 80 $s^2\sigma/K$. This is about a tenth of the horizontal speed of phase propagation, $\sigma/K$, if $s = 0.035$, for example, drift speeds of about 0.03 m s$^{-1}$ will be produced by the reflection of a wave with length $2\pi/K = 10$ km and period 10 h with horizontal speed, = length/period, of about 0.3 m s$^{-1}$. In addition to the Lagrangian drift, the Eulerian upslope currents may be significant when $\theta$ is near 180°, for example when an internal tide generated at the shelf break first reflects from the continental rise.

This study identifies several processes associated with internal wave reflection from sloping boundaries, and places bounds on the likely magnitude of the effects of rotation, which are particularly important for internal waves with near-inertial frequency. Many effects not easily studied analytically are however ignored, particularly the nonuniformity of wave trains, of the topography, and of the density field, as well as wave breaking, which in practice may prevail, if not dominate, in the process of internal wave reflection. These deserve further study, perhaps using numerical techniques (e.g., see Slinn and Riley 1998).

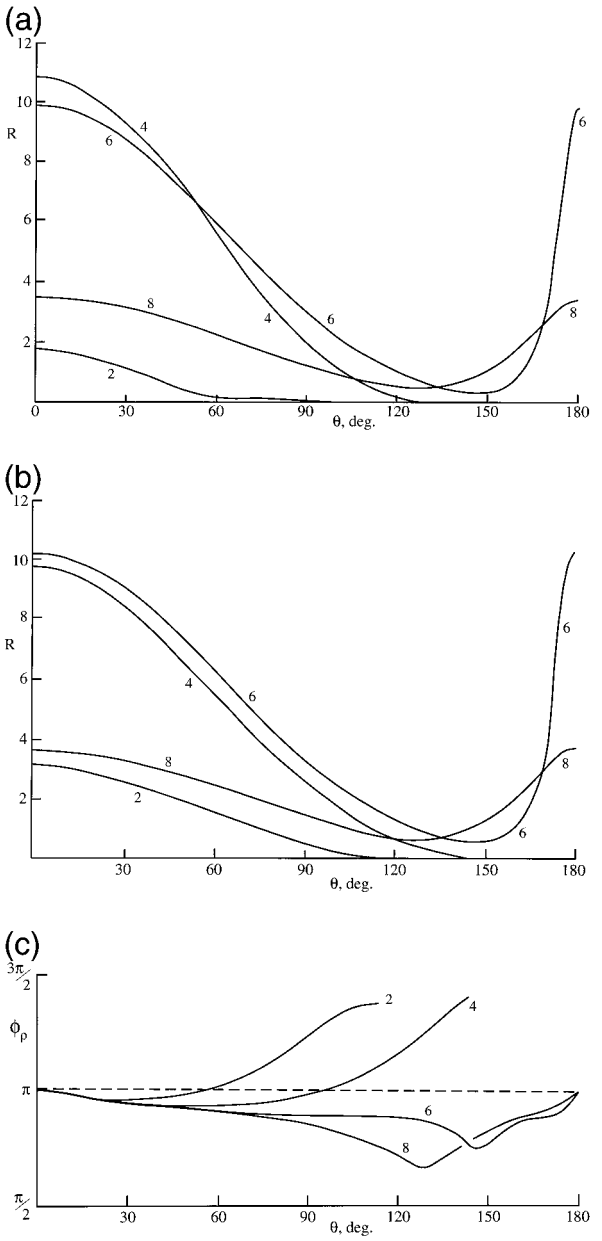


FIG. 8. The variation of the scaled second-order density variations at $\alpha = 5°$ and at various $\beta$ (labeled): (a) The ratio $R = q_2/sq_1$, when $f/N = 0$; (b) the same when $f/N = 0.1$. (c) The phase difference $\phi_\rho$ when $f/N = 0.1$. When $f/N = 0$, the corresponding phase difference is $\pi$ (dashed).

*Acknowledgments.* In August 1998 Dr. Walter Munk asked me if I knew whether the reflection of near-inertial waves from slopes could result in instability and eddying motions. While such instability is known to develop in the strong alongslope currents in the surface wave surf zone in the absence of rotation (Bowen and

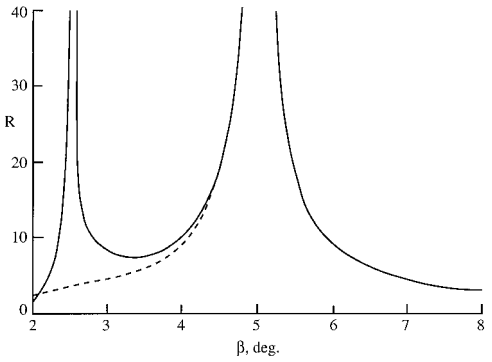


FIG. 9. The variation of the scaled ratio of second and first order density variations, $R$, with $\beta$ when $\alpha = 5°$ and $\theta = 20°$, for $f/N = 0$ (full line) and $f/N = 0.1$ (dashed). The lines overlap at $\beta > 4.5°$.

Holmam 1989 and the comparable flows produced in the ''internal surf zone'' may also be unstable, Thorpe 1998a), I realized that little was known about the effects of rotation on internal wave reflection, even when waves do not break. I am grateful for the Dr. Munk's prompt to begin to rectify this situation. An examination of mean flow generation in the presence of rotation and *wave breaking*, and of its stability once generated, remains to be done. Part of this was written during a visit to LRH, EPFL, Lausanne, Switzerland, and I am grateful for the hospitality of my friends there.

## APPENDIX A

### The Equations of Motion

The governing equations in the $(x, y, z)$ coordinates may be written as

(i) the vorticity equations in the $y$ direction,

$$\partial/\partial t(\partial u/\partial z - \partial w/\partial x) - f(c_\alpha \partial v/\partial z + s_\alpha \partial v/\partial x) + g/\rho_0(s_\alpha \partial\rho/\partial z - c_\alpha \partial\rho/\partial x) = \partial I_3/\partial x - \partial I_1/\partial z, \quad \text{(A1)}$$

and in the $z$ direction,

$$\partial/\partial t(\partial u/\partial y - \partial v/\partial x) + fc_\alpha \partial w/\partial z + fs_\alpha \partial w/\partial x + (g/\rho_0)s_\alpha \partial\rho/\partial y = \partial I_2/\partial x - \partial I_1/\partial y. \quad \text{(A2)}$$

(These equations are used in preference to the momentum equations to avoid the necessity to deal with pressure. It is assumed that the Boussinesq approximation is valid. This is not always so; see for example Thorpe 1968);

(ii) the equation of density conservation

$$\partial\rho/\partial t - (N^2/g)\rho_0 s_\alpha u - (N^2/g)\rho_0 c_\alpha w = -I_4, \quad \text{(A3)}$$

and (iii) the volume conservation equation

$$\partial u/\partial x + \partial v/\partial y + \partial w/\partial z = 0, \quad \text{(A4)}$$

where $I_1 = F(u)$, $I_2 = F(v)$, $I_3 = F(w)$ and $I_4 = F(\rho)$, and $F$ is the operator $\{u\partial/\partial x + v\partial/\partial y + w\partial/\partial z\}$ so that each of the $I$ terms is proportional to $A^2$. The density is $\rho_0[1 - N^2(xs_\alpha + zc_\alpha)/g] + \rho$, and $(u, v, w)$ are the velocity components in the $(x, y, z)$ coordinates.

## APPENDIX B

### The First-Order Solution

The solutions for the $(x, y, z)$ velocity components $(u, v, w)$ and density $\rho$, with subscripts $I$ and $R$ to indicate the incident and reflected waves, respectively, can be written $u_I = u_{sI}s_I + u_{cI}c_I$, $v_R = v_{aR}s_R + v_{sR}c_R$, etc., where $c_I = \cos(kx + ly + m_I z - \sigma t)$, $c_R = \cos(kx + ly + m_R z - \sigma t)$, and

$$u_{cI} = (ak/\gamma)(s_\beta c_\beta - s_\alpha c_\alpha r), \qquad u_{sI} = -al(c_\alpha c_\beta/s_\beta)(f/\sigma),$$

$$v_{cI} = (alc_\beta/s_\beta), \qquad v_{sI} = a(kc_\beta/\gamma)(f/\sigma)(s_\beta c_\alpha - s_\alpha c_\beta r),$$

$$w_{cI} = -akr, \qquad w_{sI} = al(c_\beta s_\alpha/s_\beta)(f/\sigma), \qquad \rho_{cI} = 0,$$

$$\rho_{sI} = -(aks_\beta N^2\rho_0/g\sigma\gamma)(s_\alpha c_\beta - s_\beta c_\alpha r), \quad \text{(B1)}$$

and

$$u_{cR} = (ak/\Omega\gamma s_\beta)[N^2 l^2 s_\alpha s_\beta[c_\alpha r(s_\beta^2 - s_\alpha^2) + s_\alpha s_\beta c_\beta + rs_\beta^2 c_\alpha] + \sigma^2\{s_\beta k^2(rs_\alpha c_\alpha + s_\beta c_\beta) + l^2[c_\beta(s_\beta^2 - s_\alpha^2) - s_\alpha^2 c_\beta - rc_\alpha s_\beta s_\alpha]\}],$$

$$u_{sR} = -a(lfc_\beta/\sigma\Omega\gamma s_\beta)[N^2 l^2 c_\alpha s_\alpha^2\gamma + \sigma^2\{k^2\{c_\alpha(s_\alpha^2 + s_\beta^2) + 2s_\alpha s_\beta c_\beta r] + l^2 c_\alpha\gamma\}],$$

$$v_{cR} = (alk^2/\gamma\Omega)\{N^2 r^2 s_\beta c_\beta\gamma + (f^2 c_\beta^2/s_\beta)[2rs_\alpha c_\alpha s_\beta + c_\beta(s_\alpha^2 + s_\beta^2 r^2)]\},$$

$$v_{sR} = (akfc_\beta/\gamma s_\beta\sigma\Omega)\{N^2 l^2 s_\alpha^2 s_\beta(c_\alpha s_\beta - rs_\alpha c_\beta) + \sigma^2[k^2 rs_\beta(s_\alpha c_\beta + rc_\alpha s_\beta) - l^2 s_\alpha(s_\alpha c_\alpha + rs_\beta c_\beta)]\},$$

$$w_{cR} = akr \qquad w_{sR} = -al(c_\beta s_\alpha/s_\beta)(f/\sigma), \qquad \rho_{cR} = -(2ak^2 N^2\rho_0 lfrs_\alpha c_\beta/g\Omega\gamma)(s_\alpha c_\beta + s_\beta c_\alpha r)$$

$$\rho_{sR} = -(ak\sigma N^2\rho_0/g\Omega\gamma)(s_\alpha c_\beta + s_\beta c_\alpha r)[k^2 r^2 s_\beta - (fls_\alpha c_\beta/\sigma)^2], \quad \text{(B2)}$$

where $\Omega = N^2k^2r^2s_\beta^2 + f^2c_\beta^2(k^2 + l^2)$, $\gamma = s_\beta^2 - s_\alpha^2$, $r^2 = (1 + l^2\gamma/k^2s_\beta^2)$, $a = \gamma A\sigma/[ks_\beta(s_\beta c_\alpha r - s_\alpha c_\beta)]$. The dispersion relation in the $(x, y, z)$ frame of reference is

$$\sigma^2 = \{N^2[(kc_\alpha - ms_\alpha)^2 + l^2] + f^2(ks_\alpha + mc_\alpha)^2\} \div (k^2 + l^2 + m^2). \quad \text{(B3)}$$

The wavenumber $(k, l, m_I)$ of the incident wave in the $(x, y, z)$ frame of reference is related to components in the horizontal and vertical directions, $K$ and $M$ respectively, by $k = Kc_\alpha c_\theta + Ms_\alpha$, $l = Ks_\theta$, $m_I = Mc_\alpha - Ks_\alpha c_\theta$. The $x$ and $y$ wavenumbers of the incident and reflected waves are the same, and the $z$ wavenumbers of the incident and reflected waves, $m_I$ and $m_R$, are $m_I = -(k/\gamma)(s_\alpha c_\alpha - rs_\beta c_\beta)$ and $m_R = -(k/\gamma)(s_\alpha c_\alpha + rs_\beta c_\beta)$, where $\gamma = s_\beta^2 - s_\alpha^2$ and $r = (1 + l^2\gamma/k^2s_\beta^2)^{1/2}$. The parameter $r$ is related to $\theta$ by

$$r = (c_\alpha s_\beta + c_\theta c_\beta s_\alpha)/(c_\theta s_\beta c_\alpha + s_\alpha c_\beta). \quad \text{(B4)}$$

## APPENDIX C

### The Second-Order Solution

The second-order components of velocity $(u_2, v_2, w_2)$ and density $\rho_2$ are found in the conventional way by solving (A1)–(A4) with the first-order solution substituted in the right-hand sides. All $I, I$ and $R, R$ products vanish because the first-order solutions are exact, leaving only $I, R$ products, which are sinusoidal in $\chi_+ = [2(kx + ly - \sigma t) + (m_I + m_R)z]$ or in $\chi_- = (m_R - m_I)z$. The latter represents the steady Eulerian currents or density perturbations which vary sinusoidally with distance $z$ from the slope with scale $2\pi/(m_I - m_R) = 2\pi\gamma/rks_\beta c_\beta$.

The Eqs. (A1)–(A4) are reduced by substitution to one equation in $w_2$. The terms that are sinusoidal in $\chi_-$ vanish identically in this equation. It has a solution that satisfies $w = 0$ at $z = 0$ of the form

$$w_2 = w_c(\cos\chi_+ - \cos\chi) + w_s(\sin\chi_+ - \sin\chi), \quad \text{(C1)}$$

where $\chi = 2(kx + ly - \sigma t) + mz$, with

$$m = -2k[s_\alpha c_\alpha + \{(1 - 4s_\beta^2)[4s_\beta^2 + (l/k)^2(4s_\beta^2 - s_\alpha^2)]\}^{1/2} \div (4s_\beta^2 - s_\alpha^2), \quad \text{(C2)}$$

and $w_c$ and $w_s$ are functions of the angles and proportional to $A^2$. The terms in (C1) that are sinusoidal in $\chi$, correspond to a wave with wavenumber $(2k, 2l, m)$ and frequency $2\sigma$ that propagates away from the boundary.

All terms in (A2) and (A4) vanish when temporal averages are taken; $w_2$ has no $\chi_-$ terms. Taking temporal averages of (A1) and integrating with respect to $z$ gives

$$(g/\rho_0)s_\alpha\Pi - fc_\alpha V = -I_1', \quad \text{(C3)}$$

where $V$ and $\Pi$ are the steady $(\chi_-)$; second-order $y$ velocity component and density variations, respectively; and $I_1'$ are the $\sin\chi_-$ and $\cos\chi_-$ terms in $I_1$, defined in appendix A. Eq. (C3) does not provide a unique solution for $V$ or $\Pi$. The terms on the right of (C3) represent a second-order geostrophic balance of the buoyancy and Coriolis forces. If it is supposed that $V = 0$, that is, the along-slope Eulerian flow is zero, then

$$\Pi = -I_1'/(g/\rho_0)s_\alpha, \quad \text{(C4)}$$

(identical to the solution at $f = 0$, except for $f$-modified terms in $I_1'$). Temporal averaging of (A3) leads to

$$U = gI_4'/N^2\rho_0 s_\alpha, \quad \text{(C5)}$$

where $I_4'$ are the $\sin\chi_-$ and $\cos\chi_-$ terms in $I_4$, and $U$ is the second-order steady $(\chi_-)$ upslope Eulerian flow. This is balanced by an opposite Stokes drift so that the mean density field remains steady in time (Thorpe 1987).

The $\chi_+$ and $\chi$ terms in $\rho_2$ are found by eliminating $u$ and $v$ in (A1)–(A4), giving two equations for $\rho_2$ in terms of the known $w_2$. Each is used, giving two separate estimates of $\rho_2$ to provide a check of the analysis and numerical programs. The sum of the periodic $\chi_+$ and $\chi$ terms can be written as $q_2 \sin[2(kx + ly - \sigma t) + \phi_{\rho 2}]$ at $z = 0$.

## REFERENCES


Bowen, A. J., and R. A. Holman, 1989: Shear instabilities of the mean longshore current 1. Theory. *J. Geophys. Res.*, **94,** 18 023–18 030.

Dunkerton, T. J., D. P. Delisi, and M.-P. Lelong, 1998: Alongslope current generated by obliquely incident internal gravity waves. *Geophys. Res. Lett.*, **25,** 3871–3874.

Eriksen, C. C., 1982: Observations of internal wave reflection off sloping bottoms. *J. Geophys. Res.*, **87,** 525–538.

——, 1985: Implications of ocean bottom reflection for internal wave spectra and mixing. *J. Phys. Oceanogr.*, **15,** 1145–1156.

——, 1998: Internal wave reflection and mixing at Fieberling Guyot. *J. Geophys. Res.*, **103,** 2977–2994.

Gill, A. E., 1982: *Atmosphere–Ocean Dynamics.* Academic Press, 662 pp.

Hogg, N. G., 1971: Longshore currents generated by obliquely incident internal waves. *Geophys. Fluid Dyn.*, **2,** 361–376.

Phillips, O. M., 1966: *The Dynamics of the Upper Ocean.* Cambridge University Press, 261 pp.

Polzin, K. L., J. M. Toole, J. R. Ledwell, and R. W. Schmitt, 1997: Spatial variability of turbulent mixing in the abyssal ocean. *Science,* **276,** 93–96.

Slinn, D. A., and J. J. Riley, 1998: Turbulent dynamics of a critically reflecting internal gravity wave. *Theor. Comput. Fluid Dyn.*, **11,** 281–304.

Thorpe, S. A., 1968: On the shape of progressive internal waves. *Philos. Trans. Roy. Soc. London,* **263A,** 563–614.

——, 1987: On the reflection of a train of finite amplitude internal waves from a uniform slope. *J. Fluid Mech.*, **178,** 279–302.

——, 1992: Thermal fronts generated by internal gravity waves reflecting from a slope. *J. Phys. Oceanogr.*, **22,** 105–108.

——, 1997: On the interactions of internal waves reflecting from slopes. *J. Phys. Oceanogr.*, **27,** 2072–2078.

——, 1998a: The generation of alongslope currents by breaking internal waves. *J. Phys. Oceanogr.*, **29,** 29–35.

——, 1998b: Some dynamical effects of internal waves and the sloping sides of lakes. *Physical Processes in Lakes and Oceans,* J. Imberger, Ed., AGU Coastal and Esturine Series, Vol. 54, Amer. Geophys. Union, 441–460.

——, 1999: Fronts formed by obliquely reflecting internal waves at a sloping boundary. *J. Phys. Oceanogr.*, **29,** 2462–2467.

Toole, J. M., R. W. Schmitt, and K. L. Polzin, 1997: Near-bottom mixing above the flanks of a midlatitude seamount. *J. Geophys. Res.*, **102,** 947–959.

Wunsch, C., 1971: Note on some Reynolds stress effects of internal waves on slopes. *Deep-Sea Res.*, **18,** 538–591.